Published in final edited form as:
Anal Chem. 2009 January 15; 81(2): 809–819. doi:10.1021/ac802096p.

Screening for DNA Adducts by Data-Dependent Constant Neutral Loss - Triple Stage (MS^3) Mass Spectrometry with a Linear Quadrupole Ion Trap Mass Spectrometer

Erin E. Bessette[1], **Angela K. Goodenough**[1,2], **Sophie Langouët**[3,4], **Isil Yasa**[1], **Ivan D. Kozekov**[5], **Simon D. Spivack**[6], and **Robert J. Turesky**[*,1]

1 *Division of Environmental Health Sciences, Wadsworth Center, New York State Department of Health, Albany, NY 12201*

2 *Bristol-Myers Squibb, P.O. Box 4000, Princeton, NJ 08543*

3 *INSERM U620, Université de Rennes I, 35043 Rennes, France*

4 *EA SeRAIC, IFR 140, 35043 Rennes, France*

5 *Department of Chemistry, Center in Molecular Toxicology, and the Vanderbilt Institute for Chemical Biology, Vanderbilt University, Nashville, TN 37235*

6 *Division of Pulmonary Medicine, Albert Einstein College of Medicine/Montefiore Medical Center, Bronx, NY 10461*

Abstract

A 2-dimensional linear quadrupole ion trap mass spectrometer (LIT/MS) was employed to simultaneously screen for DNA adducts of environmental, dietary, and endogenous genotoxicants, by data-dependent constant neutral loss scanning followed by triple-stage mass spectrometry (CNL-MS^3). The loss of the deoxyribose (dR) from the protonated DNA adducts ($[M+H-116]^+$) in the MS/MS scan mode triggered the acquisition of MS^3 product ion spectra of the aglycone adducts ($[BH_2^+]$). Five DNA adducts of the tobacco carcinogen 4-aminobiphenyl (4-ABP) were detected in human hepatocytes treated with 4-ABP, and three DNA adducts of the cooked-meat carcinogen 2-amino-3,8-dimethylimidazo[4,5-*f*]quinoxaline (MeIQx) were identified in the livers of rats exposed to MeIQx, by the CNL-MS^3 scan mode. Buccal-cell DNA from tobacco smokers was screened for DNA adducts of various classes of carcinogens in tobacco smoke including 4-ABP, 2-amino-9*H*-pyrido[2,3-*b*]indole (AαC), and benzo[*a*]pyrene (BaP); the cooked-meat carcinogens MeIQx, AαC, and 2-amino-1-methyl-6-phenylmidazo[4,5-*b*]pyridine (PhIP); and the lipid peroxidation products acrolein (AC) and *trans*-4-hydroxynonenal (HNE). The CNL-MS^3 scanning technique can be used to simultaneously screen for multiple DNA adducts derived from different classes of carcinogens, at levels of adduct modification approaching 1 adduct per 10^8 unmodified DNA bases, when 10 μg of DNA are employed for the assay.

Introduction

The covalent modification of DNA by chemical mutagens is regarded as the initiating step in chemical carcinogenesis.[1] The measurement of DNA adducts is an important endpoint, both for cross-species extrapolation of the biologically effective dose and for human risk

Corresponding Author Footnote: Robert J. Turesky, Ph.D., Division of Environmental Disease Prevention, Wadsworth Center, New York State Department of Health, Phone: 518-474-4151, Fax: 518-473-2095, Author Email Address: Rturesky@wadsworth.org.

assessments of exposure to chemical carcinogens.[2,3] The ^{32}P-postlabeling method has been a mainstay in biomonitoring of DNA adducts, because of its sensitivity and ability to detect many different classes of DNA adducts.[4] HPLC coupled with electrochemical or fluorescence detection has also been used to measure certain types of oxidative DNA lesions [5] or polycyclic aromatic hydrocarbon (PAH) adducts.[6] Immunohistochemistry (IHC) is a third technique that has been employed to monitor multiple classes of carcinogen-DNA adducts.[7] A major limitation in all of these analytical methods is the lack of information that they provide on the structure of the DNA adduct. Hence, the identity of the lesion remains equivocal.

Sensitive mass spectrometric (MS) methods have been established during the past two decades, to detect DNA adducts. These MS techniques provide varying degrees of structural information on the adduct. Accelerator mass spectrometry (AMS) is the most sensitive MS-based technique, [8] but it requires dosing the subject with a radiolabeled substrate.[9] Both tritiated and ^{14}C-isotopically labeled carcinogens have been used for adduct detection by AMS.[8] However, structural information is limited to the detection of the radioactive isotope; then a chromatographic technique and co-elution of the adduct with a non-radioactive reference compound are required to provide evidence of adduct identity. Gas chromatography-negative ion chemical ionization/mass spectrometry (GC-NICI/MS) has been used to successfully measure several classes of DNA adducts, following chemical derivatization.[10] Because only one ion is usually monitored, structural information provided about the adduct is limited. Atmospheric pressure ionization (API) techniques are the most robust analytical MS methods used to detect nonvolatile and thermally labile DNA adducts.[10-12]

Liquid chromatography in combination with electrospray ionization (ESI) tandem mass spectrometry (LC-ESI/MS/MS) has been used to analyze numerous classes of carcinogen-DNA adducts.[10,12] LC-ESI/MS with triple quadrupole tandem mass spectrometry (TQ/MS/MS) has been the primary instrumentation for the quantification of DNA adducts. For trace-analysis studies, the TQ/MS/MS system is operated in the selected reaction monitoring (SRM) scan mode. The protonated adducts ($[M+H]^+$) are selectively transmitted by the first mass analyzer (Q1) and are subjected to collision-induced dissociation (CID), typically with argon gas, in the second quadrupole (Q2). These collision conditions generally result in the loss of deoxyribose $[M+H-116]^+$, to form the protonated base aglycone adducts $[BH_2]^+$ as the principal product ions; these are then selectively transmitted through the third quadrupole (Q3). The SRM scan mode is very effective for precise quantification because of the rapid duty cycle of TQ/MS/MS. Under higher collision-energy conditions, the aglycone $[BH_2]^+$ ion undergoes extensive fragmentation, and the product ion scan mode can be used to obtain structural information about the adduct.[11] However, the slow scanning rate of the product ion scan mode generally precludes the use of this mode for characterization of DNA adducts in vivo;[13] the scanning method lacks sensitivity, because only a small fraction (<1%) of the total ions enter the MS.[14,15] Thus, in trace-analysis measurements by TQ/MS/MS, the analyst must rely solely on the characteristic retention time (t_R); often, only a single SRM transition ($[M+ H-116]^+$) is used as a criterion for analyte identification.

Quadrupole ion trap mass spectrometry (QIT/MS)[16] has been used in a variety of bioanalytical applications, including proteomics,[17] oligonucleotide sequencing,[18,19] analyses of dietary and environmental contaminants,[20] characterization of drug metabolites,[21,22] and DNA adduct measurements.[23-26] The QIT/MS permits ion storage and sequential ejection of ions, as a function of the mass, through adjustment of the strength of the quadrupole field holding the ions. This scan filter enables consecutive reaction monitoring (CRM), or multi-stage scan events (MS^n), and the rapid-scanning capacity of the instrument permits the routine acquisition of full product ion spectra, thereby enabling extensive mass spectral characterization of the analytes. The recently developed 2-dimensional LIT/MS has been advertised to have superior ion storage volume and trapping efficiencies, as well as reduced space-charge effects[27] and

increased sensitivity, in comparison to some predecessor 3-dimensional QIT/MS instruments.[28-30] We recently employed a LIT/MS to quantitate DNA adducts of PhIP,[25] an experimental animal carcinogen and likely human carcinogen,[31] that is formed in cooked meat.[32] The high ion dissociation efficiency of the LIT/MS resulted in the recovery of >90% of the total ion counts of the PhIP adducts as it transitioned from MS^n to MS^{n+1} stage scan mode, and enabled us to characterize DNA adducts of PhIP formed in experimental animals, with full scan spectra at MS^3 and MS^4 stage scan modes.[25]

LC/MS has generally been applied to the analysis of one to several DNA adducts of a specific carcinogenic agent.[33,34] However, humans are continuously exposed to genotoxicants in the environment and the diet, as well as endogenously as a consequence of oxidative cellular stress. Thus, a robust MS screening method that can simultaneously analyze multiple adducts derived from multiple sources of exposures would represent a major advance in biomonitoring of DNA adducts. There is one published report that describes the use of TQ/MS/MS and the CNL scan mode transition $[M+H]^+ \rightarrow [M+H-116]^+$, attributed to the loss of dR, to monitor putative DNA adducts in lung tissue of tobacco smokers.[35] Numerous analytes were detected; however, it was not known whether many of these analytes were actually DNA adducts or simply other compounds that lost 116 Da upon collision-induced dissociation (CID) in MS/MS. A variety of data-dependent scan techniques employing QIT/MS have been used to monitor post-translational modifications of proteins,[36] and to characterize drug metabolites.[21,22,37] The neutral-loss scan mode, by the traditional definition, cannot be performed on the LIT/MS. However, neutral loss ion maps can be obtained retrospectively from the full set of MS/MS data, once the acquisition is complete. We sought to determine whether the rapid scanning speed and high sensitivity provided by the LIT/MS can be exploited to screen for multiple DNA adducts of multiple classes of genotoxicants by data-dependent CNL-MS^3, using the neutral loss of the dR moiety in the MS/MS scan mode to trigger the acquisition of MS^3 product ion spectra of the aglycone ion $[BH_2^+]$ adducts in a single analysis.

Experimental Section

Caution:*PhIP, MeIQx, AaC, 4-ABP, BaP, HNE, AC, and their derivatives are genotoxic and/or carcinogenic agents, and they should only be handled in a well-ventilated fume hood with the appropriate protective clothing.*

Chemicals

MeIQx and PhIP were purchased from Toronto Research Chemicals (Toronto, ON, Canada). 2-Nitro-9*H*-pyrido[4,5-*b*]indole (NO_2-AαC) was a kind gift from Dr. D. Miller, NCTR (Jefferson, AR). (±)-*r*-7,*t*-8-Dihydroxy-*t*-9,10-epoxy-7,8,9,10-tetrahydrobenzo[*a*]pyrene ((±)(*anti*)B[*a*]PDE)) was purchased from the NCI Chemical Carcinogen Reference Standards Repository, Midwest Research Institute (Kansas City, MO). Calf thymus (CT) DNA, deoxyguanosine (dG), DNase I (Type IV, bovine pancreas), alkaline phosphatase (from *E. coli*), and nuclease P1 (from *Penicillium citrinum*) were purchased from Sigma (St. Louis, MO). [$^{13}C_{10}$]dG was purchased from Cambridge Isotopes (Andover, MA). Phosphodiesterase I (from *Crotalus adamanteus* venom) was purchased from GE Healthcare (Piscataway, NJ). All solvents used were high-purity B & J Brand from Honeywell Burdick and Jackson (Muskegon, MI). ACS reagent-grade formic acid (88%) was purchased from J.T. Baker (Phillipsburg, NJ). Hypersep™ filter SpinTips C-18 (20 mg) were acquired from Thermo Scientific (Palm Beach, FL).

Preparation of the DNA adduct standards

N-(deoxyguanosin-8-yl)-PhIP (dG-C8-PhIP),[25,38] *N*-(deoxyguanosin-8-yl)-MeIQx (dG-C8-MeIQx) and 5-(deoxyguanosin-N^2-yl)-MeIQx (dG-N^2-MeIQx),[13,39] and *N*-

(deoxyguanosin-8-yl)-2-amino-9*H*-pyrido[2,3-*b*]indole (dG-C8-AαC)[40] were prepared by reaction of their *N*-acetoxy HAA derivatives with dG or [$^{13}C_{10}$]dG (5 mg) in 100 mM K_2HPO_4 buffer (pH 8.0). *N*-(deoxyguanosin-8-yl)-4-aminobiphenyl (dG-C8-ABP) was prepared by reaction of *N*-hydroxy-4-ABP with pyruvonitrile, followed by reaction with dG or [$^{13}C_{10}$]dG.[41] The (±)-*anti*-B[a]PDE-derived dG adducts, 10-(deoxyguanosin-N^2-yl)-7,8,9-trihydroxy-7,8,9,10-tetrahydrobenzo[*a*]pyrene (dG-N^2-BaP) were prepared by reaction of (±)-*anti*-B[a]PDE with dG as described.[42] The adducts were purified by SPE followed by HPLC purification,[13,39] and were isolated as a mixture of unresolved isomers. The (6*R*/*S*)-3-(2′-Deoxyribos-1′-yl)-5,6,7,8-tetrahydro-6-hydroxypyrimido[1,2-*a*]purine-10(3*H*)one (6-hydroxy-PdG),[43] the (8*R*/*S*)-3-(2′-deoxyribos-1′-yl)-5,6,7,8-tetrahydro-8-hydroxypyrimido [1,2-*a*]purine-10(3*H*)one (8-hydroxy-PdG),[44] and the isomeric 1,N^2-8-hydroxypropano-2′-deoxyguanosine adducts of HNE (dG-HNE)[45] were synthesized as previously reported.

PhIP-modified calf thymus DNA

[^{3}H]-PhIP-modified CT DNA was provided by Dr. F. Kadlubar (UAMS, Little Rock, AR).[38] The extent of PhIP modification was estimated at 1 adduct per 10^6 unmodified DNA bases.

4-ABP- and BaP-modified calf thymus DNA

[^{3}H]-4-ABP-CT DNA (62 adducts per 10^8 unmodified DNA bases)[46] and [^{3}H]-BaP-modified CT DNA (111 adducts per 10^8 unmodified DNA bases)[47] were provided by Dr. F. Beland (NCTR, Jefferson, AR).

DNA adduct formation of 4-ABP in human hepatocytes

A human liver sample was obtained from a patient undergoing liver resection for primary hepatoma via the Biological Resource Center (CHRU Pontchaillou, Rennes, France). The research protocol met French legal guidelines and the requirements of the local institutional ethics committee. Hepatocytes were isolated by a two-step collagenase perfusion procedure.[48] The liver parenchymal cells were seeded, at a density of 10^6 viable cells/35-cm^2 dish, in 2 ml of Williams' medium with supplements.[48] Once the medium was renewed, 4-ABP (10 μM) in DMSO (0.1% v/v) was added and the cells were incubated for 24 h. Cellular DNA was isolated by a chloroform/phenol extraction method.[4]

Animal treatment with MeIQx

Male Fischer-344 rats (220-260 g of body wt, Iffa Credo, L'Abresle, France) were dosed orally with MeIQx-HCl (10 mg/kg body wt) in 10 mM phosphate-buffered saline (pH 7.4).[13] Control animals received phosphate-buffered saline. The animals were sacrificed 24 h after treatment and liver DNA was isolated as previously described.[13]

Human buccal cells

Subjects (tobacco smokers >20 cigarettes per day, and on a non-controlled diet), swished mouthwash (Scope brand, 10 mL) vigorously for 1 min and then expelled it into a 50-ml polypropylene Falcon tube. The biospecimens were rendered anonymous and stored at -20 °C until processed. DNA was isolated by phenol/chloroform extraction as previously described.[49] This study was approved by the Institutional Review Boards at the Wadsworth Center and the Albert Einstein College of Medicine.

Enzyme digestion and solid phase extraction (SPE) of DNA adducts

The enzymatic digestion conditions used for the hydrolysis of DNA employed DNAse I for 1.5 h, followed by incubation with nuclease P1 for 3 h and then alkaline phosphatase and

phosphodiesterase for 18 h. Thereafter, three volumes of cold C_2H_5OH (200 proof) were added to the hydrolysis mixture.[25]

SPE DNA adduct enrichment procedure

The C_2H_5OH/DNA digest solution was centrifuged at 15,000 *g* for 2 min. The supernatant containing DNA adducts was removed and dried by vacuum centrifugation. Samples were purified by SPE, using SpinTips. The DNA digest extracts were resuspended in 10% CH_3OH in 0.1% HCO_2H (0.25 mL) and applied to a SpinTip, which was placed into a vacuum manifold. The SpinTip was then washed with 10% CH_3OH in 0.1% HCO_2H (2 × 0.25 mL), to remove non-modified 2′-deoxynucleosides. For studies designed to screen for 6- and 8-hydroxy-PdG, the SpinTip was washed with 0.1% HCO_2H (2 × 0.25 mL). The desired adducts were eluted with CH_3OH containing 0.1% HCO_2H (0.2 mL) into silylated glass insert capillary LC vials (Microliter Analytical Supplies, Suwanee, GA). Samples were evaporated to dryness by vacuum centrifugation and reconstituted in 1:1 DMSO/H_2O (20 μL).

LC/MS Parameters

Chromatography was performed with an Agilent 1100 Series capillary LC system (Agilent Technologies, Palo Alto, CA) equipped with an Aquasil C18 column (0.32 × 250 mm) from Thermo Fisher (Bellafonte, PA). Samples (2 μL) were injected, and analytes were separated with a gradient. The solvent conditions were held at 100% A (solvent composition: 0.01% HCO_2H and 10% CH_3CN) for 2 min, followed by a linear gradient to 100% B (solvent composition: 95% CH_3CN containing 0.01% HCO_2H) over 30 min at a flow rate of 6 μL/min. The MS instrumentation was an LTQ mass spectrometer (ThermoElectron, San Jose, CA). The Xcalibur Version 2.07 software was used for data manipulations. Analyses were conducted in the positive ionization mode and employed an Advance nanospray source from Michrom Bioresource Inc. (Auburn, CA). Representative optimized instrument tuning parameters were as follows: capillary temperature 225 °C; source spray voltage 3.5 kV; source current 2.8 μA; no sheath gas, sweep gas or auxiliary gas was employed; capillary voltage 40 V; tube lens voltage 110 V; and in-source fragmentation 10 V. The normalized collision energies were set at 24 and 34, and the isolation widths were set at 4.0 and 1.5 Da, respectively, for the MS^2 and MS^3 scan modes. The activation Q was set at 0.35 and the activation time was 30 msec. Helium was used as the collision damping gas in the ion trap and was set at a pressure of 1 mTorr. One μscan was used for data acquisition. The automatic gain control (AGC) settings were full MS target 30,000 and MS^n target 10,000, and the maximum injection time was 50 ms.

CNL-MS^3 data dependent scanning

A signal threshold of 200 counts was required in full-scan MS $[M+H]^+$ and MS/MS $[M+H-116]^+$ scan modes to trigger the acquisition of the MS^3 scan. The instrument scanned from 300 to 600 Da in MS full scan mode, and from 100 to 600 Da in CRM scan modes. A window of 116 ± 0.5 Da was used to monitor the loss of the dR moiety. The top 4 or 7 ions were monitored in MS/MS. For some studies, a mass list was used, to monitor specific DNA adducts. The MS^3 scan mode was triggered if the aglycone adduct $[M+H-116]^+$ was within the top 10 most abundant fragment ions in the MS/MS product ion spectrum.

Results and Discussion

The efficacy of the data-dependent CNL-MS^3 scan mode to detect DNA adducts was evaluated with DNA samples obtained from rat liver and human hepatocytes exposed to a single carcinogenic agent, and from buccal cell DNA samples collected from individuals who are exposed to numerous carcinogenic agents in tobacco smoke and the diet.[32,50] We monitored DNA adducts of aromatic amines, HAAs, PAHs, and aldehydes that form in tobacco smoke (4-ABP, AαC, PhIP, BaP, and AC);[50-52] DNA adducts of HAAs formed in cooked meats

(PhIP, MeIQx, AαC)[32] and α,β-unsaturated aldehydes (AC, HNE), which are produced endogenously through lipid peroxidation as a consequence of oxidative stress.[53] The structures of the DNA adducts investigated are shown in Figure 1 (The chemical structures of the carcinogens are provided in Supporting Information, Figure S-1).

We evaluated the sensitivity and specificity of the data-dependent CNL-MS^3 scan mode to detect adducts in global scanning or with the use of a targeted adduct ion mass list. The monitoring of DNA adducts in the global scan mode is an intensity-dependent MS/MS experiment; MS/MS acquistion is carried out on the most abundant ions detected in the full-scan mode. With the use of a targeted mass-list, the MS/MS acquisition is automatically triggered once a listed adduct ion is detected. The loss of the neutral dR fragment moiety in the MS/MS scan mode $[M+H-116]^+$ is used to activate the acquisition of the MS^3 product ion spectra of the aglycone ion $[BH_2^+]$.

4-ABP-DNA Adduct Formation in Human Hepatocytes

In the first application, we have assayed DNA adduct formation in cultured human hepatocytes exposed to 4-ABP (10 μM). This aromatic amine arises in tobacco smoke;[51] it is an experimental animal carcinogen and a human urinary bladder carcinogen.[54] The major adduction product of 4-ABP occurs at the C8 atom of dG and the *N*-hydroxylated amine group of 4-ABP, to produce dG-C8-ABP.[54] Two other isomeric dG adducts have been characterized: a hydrazo linked adduct, *N*-(deoxyguanosin-N^2-yl)-4-aminobiphenyl (dG-N^2-N^4-ABP); and an adduct formed at the N^2 atom of dG and the C-3 atom of 4-ABP, 3-(deoxyguanosin-N^2-yl)-4-aminobiphenyl (dG-N^2-ABP).[54,55] The dA adduct has been identified as *N*-(deoxyadenosin-8-yl)-4-aminobiphenyl (dA-C8-ABP)[55] (Figure 1).

Adducts of 4-ABP formed in hepatocytes were monitored by scanning of the protonated ions $[M+H]^+$ from the mass range of 400 to 500 Da, a range that encompasses the molecular masses of all known adducts of 4-ABP. The mass chromatograms of putative adducts in the full-scan, MS/MS, CNL $[M+H-116]^+$, and the data-dependent CNL-MS^3 scan modes are presented in Figure 2. The chromatograms in the full-scan and MS/MS scan modes are complex. Processing of the MS/MS data set with the CNL $[M+H-116]^+$ and data-dependent CNL-MS^3 filters considerably reduced background signals and the number of detected peaks, resulting in greatly simplified mass chromatograms. Three presumed DNA adducts, which are minor constituents of the DNA digest, are detected in treated hepatocytes but not in the control hepatocytes, when the CNL $[M+H-116]^+$ and CNL-MS^3 scan mode filters are employed to process the data.

The masses of two compounds were observed at *m/z* 435 $[M+H]^+$, a molecular mass consistent with an adduct formed from the reaction of dG with HONH-ABP. The third adduct displayed an ion at *m/z* 419 $[M+H]^+$, a molecular mass consistent with a reaction product formed between dA and HONH-ABP. The major adduct was identified as dG-C8-ABP (t_R = 21.4 min), on the basis of its MS^3 product ion spectrum, and its co-elution with the isotopically labeled $[^{13}C_{10}]$ dG-C8-ABP (added prior to the DNA digest at a level of 5 adducts per 10^8 DNA bases; data not shown). On the basis of the response of the signal of the dG-C8-ABP relative to $[^{13}C_{10}]$ dG-C8-ABP, the amount of dG-C8-ABP formed was estimated to be at about 9.7 adducts per 10^6 DNA bases. Under the assumption that the ABP adducts display similar ionization and dissociation efficiencies, when analyzed by LIT/MS, the levels of the isomeric dG-ABP adduct (t_R = 19.2 min) and the dA-ABP adduct (t_R = 23.9 min) were ~10-fold lower levels than those of the dG-C8-ABP adduct. Eight MS^3 scans were acquired across the peak of dG-C8-ABP, and four MS^3 scans were acquired across the peaks of the isomeric dG-ABP adduct and the dA-ABP adduct with CNL-MS^3, using global scanning.

The proposed structures of the adducts and the assignments of the fragment ions and neutral losses in the MS^3 and MS^4 stage spectra of 4-ABP dA and dG adducts (Figure 3) are tentative.

There are several possible isomeric adduct structures that could undergo fragmentation to produce these product ions. An unambiguous elucidation of the structures of the adducts would require exact mass measurements of the fragment ions, in conjunction with NMR spectroscopy. The assigned structure of dG-C8-ABP is supported by the MS^3 product ion spectra of the aglycone guanyl-C8-ABP (*m/z* 319.1) $[BH_2]^+$ (Figure 3A). Many of the product ions were previously characterized by TSQ/MS/MS, and are attributed to fragmentation of the guanyl moiety.[56] The product ion formed at *m/z* 195 $[BH_2-124]^+$ (loss of $C_4H_4N_4O$), occurs through cleavage of the *N*7-C8 and C4-*N*9 bonds of the guanine base. This mechanism of fragmentation is shared by many dG-C8-AA and dG-C8-HAA adducts.[11,23,57] However, the ion is produced at relatively low abundance in the MS^3 product ion spectrum of dG-C8-ABP, as compared to the corresponding fragment ion observed in the MS^3 product ion spectrum of dG-C8-PhIP[25] or dG-C8-MeIQx (*vide infra*). The second-generation product ions of guanyl-4-ABP at *m/z* 277.2 $[BH_2-42]^+$ and *m/z* 249.2 $[BH_2-70]^+$ underwent fragmentation at MS^4, to produce the ion at *m/z* 195.2 as a prominent product ion (Supporting Information, Figure S-2).

Both dG-N^2-N^4-ABP and dG-N^2-ABP are plausible structures of the isomeric dG adduct (t_R = 19.2 min). The MS^3 product ion spectrum of the aglycone $[BH_2]^+$ at *m/z* 319.3 displays a prominent fragment ion at *m/z* 302, due to loss of NH_3 and several less abundant product ions (Figure 3B). Both guanyl-N^2-N^4-ABP and guanyl-N^2-ABP adducts can be expected to undergo cleavage of the guanyl moiety to produce these fragment ions. The structure of the adduct was tentatively assigned as the dG-N^2-N^4-ABP isomer, on the basis of the MS^4 product ion spectrum of the second-generation product ions of the charged species at *m/z* 210.3 $[BH_2\text{-}109]^+$ ($C_4H_3N_3O$) (Supporting Information, Figure S-3 and Scheme S-1). The fragment ion at *m/z* 141.1 $[BH_2\text{-}109\text{-}69]^+$ ($C_2H_3N_3$) can be formed by cleavage of the aniline ring at the C4 atom of 4-ABP in the guanyl-N^2-N^4-ABP adduct, but this product ion seems unlikely to arise from guanyl-N^2-ABP at the MS^4 scan stage. The unambiguous characterization and definitive identification of this adduct structure, by MS, will require a synthetic adduct with stable ^{13}C or ^{15}N isotopes at defined positions of the molecule.

The MS^3 product ion spectrum of the dA-C8-ABP adduct supports the assigned structure that has a linkage between the C8 atom of dA and the 4-NH_2 group of 4-ABP (Figure 3C). The MS^3 product ion spectrum aglycone $[BH_2]^+$ adduct at *m/z* 303.3 displays several fragments of the adenine moiety. The product ion at *m/z* 195.2 $[BH_2\text{-}108]^+$ ($C_4H_4N_4$) is proposed to occur via cleavage of the *N*7-C8 and *N*9-C4 bonds, to produce the protonated 4-ABP containing a CN moiety. The second-generation product ions of adenyl-4-ABP adduct at *m/z* 276.2 $[BH_2\text{-}27]^+$ (HCN) underwent fragmentation at the MS^4 stage to produce the 195.2 ion as the base peak in the product ion spectra (Supporting Information, Figure S-4).

4-ABP-DNA adduct formation in human hepatocytes was further investigated through the use of the CNL-MS^3 scan mode with a targeted mass list of adducts of dG-ABP at *m/z* 435.2 and dA-ABP at *m/z* 419.2. The CNL-MS^3 dependent scan mode with the use of a targeted mass list provided coverage of 4-ABP adducts that was superior to the coverage of the global scanning mode: the number of MS^3 product ion spectra acquired across the peaks doubled for dG-C8-ABP and tripled for dG-N^2-ABP and dA-C8-ABP. Two additional isomeric dA-ABP adducts were detected (t_R = 17.6 and 22.6 min) (Supporting Information, Figure S-5). The MS^3 product ion spectra of the aglycones $[BH_2]^+$ are presented in Supporting Information Figure S-6). The structures of these adducts remain to be determined.

MeIQx DNA Adduct Formation in Rat Liver

In the second application, we explored the efficacy of the data-dependent CNL-MS^3 scan mode, in detecting DNA adducts in the livers of rats treated with MeIQx. This HAA, which is formed in cooked beef, is a potent bacterial mutagen and an experimental animal carcinogen.[32] Two isomeric dG adducts *N*-(deoxyguanosin-8-yl)-MeIQx (dG-C8-MeIQx) and 5-(deoxyguanosin-

N^2-yl)-MeIQx (dG-N^2-MeIQx) have been reported to form by reaction of *N*-acetoxy-MeIQx with dG or DNA (Figure 1).[39] These adducts also have been identified in rats treated with MeIQx.[13] Global and targeted mass $[M+H]^+$ list scanning modes were employed to screen for putative adducts of MeIQx formed with dC (*m/z* 439.2), dT (*m/z* 454.2), and dA (*m/z* 463.2), as well as with dG (*m/z* 479.1). The dG-C8-MeIQx adduct (t_R = 20.1 min), previously estimated in these liver samples at 1.8 ± 0.5 adducts per 10^7 DNA bases, by TQ/MS/MS,[13] was detected by global scanning with CNL-MS^3 (four MS^3 scans acquired across the peak; data not shown). The dG-N^2-MeIQx adduct, previously estimated at 1.4 ± 0.3 adducts per 10^7 DNA bases in these DNA samples,[13] was not found here, under global scanning conditions. However, when the targeted mass list was employed for screening of adducts, dG-C8-MeIQx (12 MS^3 scans acquired across the peak), as well as dG-N^2-MeIQx (t_R = 15.8 min) (6 MS^3 scans acquired across the peak), and a previously unreported dA adduct of MeIQx (t_R = 17.6 min) (7 MS^3 scans acquired across the peak) were easily identified. The mass chromatograms for adducts in full-scan, MS/MS, CNL ($[M+H-116]^+$), and data-dependent CNL-MS^3 scan modes of the targeted mass list are presented in Figure 4. The high background signals precluded the detection of these adducts in the full-scan and MS/MS-scan modes, but all three adducts are observed, when the CNL ($[M+H-116]^+$ and CNL-MS^3 filters are employed for data analysis. The response of synthetic dG-N^2-MeIQx was 10-fold lower than the response of dG-C8-MeIQx under these CID conditions, a fact which explains the relatively weaker signal of dG-N^2-MeIQx in the DNA samples. We surmise that the dA-MeIQx adduct is present in rat liver DNA at a level of several adducts per 10^8 unmodified DNA bases.

The MS^3 product ion spectra acquired by the CNL-MS^3 scan mode and the proposed mechanisms of fragmentation of the isomeric dG-C8-MeIQx and dG-N^2-MeIQx adducts, and of the dA adduct, are presented in Figure 5. The product ion spectra of dG-MeIQx adducts, acquired by TQ/MS/MS, were previously described.[11,13] Many of the same product ions are observed with the LIT/MS. The MS^3 product ion spectra of dA-MeIQx aglycone $[BH_2]^+$ at *m/z* 347.3 (Figure 5C) provided rich structural information about the structure of the adduct. Bond formation is proposed to occur between the N^6 atom of adenine and the C-5 atom of the MeIQx heteronucleus, to form 5-(deoxyadenosin-N^6-yl)-MeIQx (dA-N^6-MeIQx) via a carbenium ion intermediate of *N*-acetoxy-MeIQx.[39] The MS^3 product ion reveals extensive fragmentation of the adenine molecule. Characteristic fragment ions arising through cleavage of adenine at the C5-C6 and *N*1-C2 bonds, or at the C5-C6 and C6-*N*1, produce protonated MeIQx containing a cyanamide moiety at *m/z* 254.3 $[BH_2\text{-}93]^+$ ($C_4H_3N_3$) or a cyano moiety at *m/z* 239.2 $[BH_2\text{-}108]^+$ ($C_4H_4N_4$); both moieties are attached to the C-5 atom of the MeIQx heteronucleus. Recently, a dA-N^6 adduct of the structurally related HAA, 2-amino-3-methylimidazo[4,5-*f*]quinoline (IQ), was identified in CT-DNA, by high resolution QIT/MS.[58] Many of the pathways of fragmentation of the dA-N^6-MeIQx and dA-N^6-IQ adducts are remarkably similar.

DNA Adduct Formation in Buccal Cell DNA of Tobacco Smokers

In the third example, we have examined the efficacy of the data-dependent CNL-MS^3 scan mode, to screen for multiple classes of DNA adducts in buccal-cell DNA from tobacco smokers. The oral and nasal cavities are the first portals of entry for genotoxicants present in diet and tobacco smoke. There are more than 60 known carcinogens present in cigarette mainstream smoke,[50] and ^{32}P-postlabeling studies have shown that a plethora of adducts are present in DNA of the oral mucosa of smokers and non-smokers alike.[59] We conducted data-dependent CNL-MS^3 monitoring of DNA adducts derived from several ubiquitous genotoxicants that occur in tobacco smoke or grilled meats, or that form endogenously, as by-products of cellular oxidative stress. AC and HNE, highly reactive α,β-unsaturated aldehydes, are formed endogenously through lipid peroxidation.[53] AC also arises in cigarette smoke at relatively high levels, ranging from 18 to 98 μg per cigarette.[60] Other tobacco genotoxicants studied here are

present at much lower levels in tobacco. AαC occurs at levels up to 258 ng per cigarette,[61] while the amounts of 4-ABP, PhIP, and BaP range between 2 and 15 ng/cigarette.[51,62] Although MeIQx has not been detected in tobacco smoke, it, along with PhIP, is formed in well-done cooked meats at the low parts-per-billion levels.[32] The expression of mRNA and catalytic activities of P450 enzymes, which bioactivate 4-ABP, BaP, and HAAs, have been detected in buccal cells,[63-65] leading us to believe that these carcinogens can form DNA adducts in buccal cells.

Buccal-cell DNA samples were spiked with 6-hydroxy-PdG, 8-hydroxy-PdG, dG-HNE, dG-C8-MeIQx, and dG-C8-AαC as monomeric adducts. dG-C8-PhIP, dG-C8-ABP, and dG-N^2-BaP were added as carcinogen-modified CT-DNA. All of the adducts were added at a level of 5 adducts per 10^8 DNA bases into a final quantity of 100 μg buccal cell DNA. Spiking of buccal-cell DNA with these adducts enabled us to confirm the efficiency of enzyme hydrolysis of carcinogen-modified CT-DNA, and the recovery of DNA adducts, and to assess the limit of detection (LOD) of the method.

The reconstructed ion mass chromatograms of DNA adducts in buccal-cell samples mined by the data-dependent CNL-MS^3 scan filter are presented in Figure 6, panel A (spiked samples) and panel B (unspiked samples). All of the adducts spiked into the buccal DNA were detected, and high-quality MS^3 product ion spectra were acquired (Figure 7). In the unspiked DNA samples, only the 6- and 8-hydroxy-PdG adducts were unequivocally identified. The number of MS^3 scans across the peaks in the spiked DNA samples ranged from 6 scans for dG-N^2-BaP to more than 30 scans for the 6- and 8-hydroxy-PdG adducts. The response of the signal for the 6- and 8-hydroxy-PdG adducts (t_R between 17 - 18 min) was 10 - 50-fold greater than the response of any other adduct (Figure 6A); the response also exceeded the signal of the pure standards spiked into the DNA by 15-fold. Indeed, high levels of 6- and 8-hydroxy-PdG adducts were detected in the unspiked buccal DNA of tobacco smokers (Figure 6, panel B).

The 6- and 8-hydroxy-PdG adducts exist as mixtures of epimers,[66] which are not completely resolved under these chromatographic conditions. The 6-hydroxy-PdG adduct elutes first and is the minor component of the mixture. The isomers are distinguished on the basis of their MS^3 product ion spectra (Figure 7).[60] The fragment ion at *m/z* 164.1 $[BH_2 - 44]^+$ (C_2H_4O), due to loss of ethenol, is only seen in the MS^3 product ion spectrum of 8-hydroxy-PdG.[60] The MS^3 product ion spectra of 6- and 8-hydroxy-PdG acquired from the unspiked samples were in excellent agreement (data not shown). The 6- and 8-hydroxy-PdG adducts were estimated at levels of above 5 adducts per 10^7 unmodified DNA bases in buccal cell DNA. These levels are similar to those levels previously measured in gingival tissue of tobacco smokers by ^{32}P-postlabeling.[67] Relatively high levels of 6- and 8-hydroxy-PdG also have been identified in human lung[35,60] and brain,[68] by LC/MS.

There are four diastereomers of dG-HNE,[66] three of which are resolved under the current chromatographic conditions. The aglycone of dG-HNE $[BH_2]^+$ at *m/z* 308.2 undergoes dehydration at the MS^3 scan stage, to produce the ion at *m/z* 290.2 $[BH_2-18]^+$ as the base peak. A second product ion at *m/z* 152 $[BH_2-156]^+$ ($C_9H_{16}O_2$) is attributed to cleavage of the HNE moiety. The occurrence of dG-HNE in unspiked buccal cell DNA is suggested by the two CNL-MS^3 scans acquired on the peak at t_R 25.6 min (Figures 6B); however, the signal is weak and identification of the adduct is equivocal.

There are four isomeric dG-N^2-BaP adducts,[42] which are partially resolved. The aglycone of dG-N^2-BaP $[BH_2]^+$ (*m/z* 454), undergoes fragmentation at the MS^3 scan stage, to produce the fragment ion at *m/z* 303 $[BH_2\text{-}151]^+$ ($C_5H_5N_5O$), due to loss of guanine, and ions at *m/z* 285 $[BH_2 - 169]^+$ ($C_5H_7N_5O_2$) and *m/z* 257 $[BH_2\text{-}197]^+$ ($C_6H_7N_5O_3$), attributed to loss of guanine and H_2O, followed by the expulsion of CO.[42,47] CNL-MS^3 spectra were also successfully

acquired on dG-C8-ABP, dG-C8-MeIQx, dG-C8-PhIP, and dG-C8-AαC in spiked buccal-cell DNA. The CNL-MS^3 product ion spectra of dG-C8-PhIP and dG-C8-AαC are shown in Figure 7. The product ion spectra of all these adducts display all of the fragment ions and at the same relative abundances that are observed for the synthetic standards.

Putative DNA adducts of 4-ABP and BaP have been detected in oral mucosa of smokers and non-smokers, when assayed by immunohistochemistry (IHC), at levels above 1 adduct per 10^7 unmodified DNA bases.[69,70] In this present pilot study of six smoking subjects, we have yet to unequivocally identify these lesions by LIT/MS (Figure 6, panel B), even though our LOD (< 5 adducts per 10^8 DNA bases) is lower than the LOD reported by IHC. We suspect that the IHC technique is detecting a variety of lesions in addition to or other than dG-C8-ABP or dG-N^2-BaP adducts.[69,70] Since LC-ESI-MS is a concentration-dependent detector,[71] the use of liquid chromatography columns with smaller inner diameters and lower flow rates should further lower the LOD of adducts detected by the CNL-MS^3 scan mode.

Scanning parameters that influence CNL-MS^3 data acquisition and the LOD

An ultra-low ion abundance of two hundred counts was chosen as the threshold in signal to trigger MS/MS and CNL-MS^3 scan events and provided the maximum number of MS^3 scans across the peaks. The CNL-MS^3 scan event was initiated only if the aglycone adduct $[M+H-116]^+$ was within the top 10 most abundant fragment ions in the MS/MS product ion spectrum. Restriction of the $[M+H]^+ \rightarrow [M+H\text{-}116]^+$ transition to the top 2 or 3 most abundant ions in the MS/MS spectrum served to increase the number of scans acquired across the peaks for some DNA adducts present at levels above 2 adduct per 10^7 bases, but this level of stringency can also diminish the number of data-dependent CNL-MS^3 scans or can even result in the omission of adducts that are present at low abundance. Remarkably, the CNL-MS^3 scan mode, used with a MS/MS tolerance of 0.5 Da, was relatively selective and few spurious peaks were detected in any of our DNA samples under these scanning parameters.

At high levels of DNA modifcation (>2 adducts per 10^7 bases), the response of adducts in MS and MS/MS scan modes are well above the background signals in the global scanning mode, and the efficiency of the data-dependent CNL-MS^3 scan mode is high: almost every MS/MS scan that produced the neutral fragment loss of 116 Da triggered the acquistion of the MS^3 product ion scan. However, at lower levels of adduct modification, when the background signal is relatively high, adducts can be overlooked in the global scan mode. The use of a targeted mass list, instead of global scanning, provides superior coverage of the adducts and results in a 2- to 3-fold increase in the number of MS^3 scans acquired across the peaks. Moreover, the post-acquisition mining of the MS/MS data with $[M+H-116]^+$ and CNL-MS^3 scan filters allowed us to identify other DNA adducts present at low abundance for both 4-ABP and MeIQx for which we did not possess standards. Two previously unreported dA adducts of 4-ABP, a novel dA adduct of MeIQx, and the isomeric dG-N^2-MeIQx adduct were identified with CNL-MS^3, when a mass list was employed for screening.

The data-dependent CNL-MS^3 scan mode used with a targeted mass list was about 5-fold less sensitive than the MS/MS^3 scan mode. However, the CNL-MS^3 filter provided simpler chromatograms with a higher signal-to-noise ratio than does the MS/MS^3 scan mode that can often result in the detection of numerous peaks. The use of reconstructed chromatograms of selected ions of MS/MS^3 data improves the signal-to-noise for DNA adducts, but the selection of ions requires prior knowledge about the identity and structure of the adduct, and the mechanisms of fragmentation.[25,72] The number of scans acquired across the peaks in the CNL-MS^3 scan mode with a targeted mass list also is greater than the number of scans acquired by MS/MS^3, when six or more adducts are monitored in the same segment of the MS/MS^3 scan mode, and provides superior MS^3 product ion spectral data. The mass list can be expanded to

at least 12 adducts without effective diminution of the number of CNL-MS^3 scans acquired across the peaks.

Conclusions

The rapid duty cycle and high sensitivity of the LIT/MS instrument permits simultaneous screening for an array of DNA adducts having diverse structures, using the data-dependent CNL-MS^3 scan mode. The MS^3 spectra of adducts can be acquired at levels of DNA modificaton below 5 adducts per 10^8 DNA bases, with 10 μg of DNA assayed on the column. The ability to screen for multiple adducts of different classes of carcinogens and to acquire MS^3 product ion spectra for proof of adduct identity in a single chromatographic run, represent major advances in MS-based DNA adduct screening techniques,[11,12] The data-dependent CNL-MS^3 scan mode is a powerful post-acquisition data-mining technique, for discovery and structural elucidation of DNA adducts, a technique which may be used in preclinical drug safety assessment.[73] With further refinements, this scanning technique can have important applications in human biomonitoring of genotoxicants.

Supplementary Material

Refer to Web version on PubMed Central for supplementary material.

Acknowledgements

The project was supported by grant R21ES-014438 (RJT, EEB, IY) and Program Project grant PO1ES-05355 (IDK, RJT) from the National Institute of Environmental Health Sciences, grant R01CA-122320 from the National Cancer Institute (RJT), and grants from the Ligue Contre le Cancer (the Cote d'armor, Morbihan and Maine et Loire committees) and the Région Bretagne, France (SL). The content is solely the responsibility of the authors and does not necessarily represent the official views of the National Cancer Institute, the National Institute of Environmental Health Sciences, the National Institutes of Health, the French Cancer Societies, or Bristol-Myers Squibb. The advice of Dr. Bill Mahn (Thermo Fisher) on the data-dependent CNL-MS^3 analyses is greatly appreciated. We thank Dr. Paul Vouros, Northeastern University; Dr. Carmelo Rizzo, Vanderbilt University; and Dr. Dieter Drexler, Bristol-Myers Squibb, for their comments on this manuscript.

References

1. Miller EC. Cancer Res 1978;38:1479–1496. [PubMed: 348302]
2. Swenberg JA, La DK, Scheller NA, Wu KY. Toxicol Lett 1995;82-83:751–756. [PubMed: 8597138]
3. Poirier MC, Beland FA. Chem Res Toxicol 1992;5:749–755. [PubMed: 1489923]
4. Beach AC, Gupta RC. Carcinogenesis 1992;13:1053–1074. [PubMed: 1638670]
5. Floyd RA, Watson JJ, Wong PK, Altmiller DH, Rickard RC. Free Radic Res Commun 1986;1:163–172. [PubMed: 2577733]
6. Jankowiak R, Small GJ. Anal Chem 1989;61:1023A–1024A. [PubMed: 2729598]
7. Poirier MC, Santella RM, Weston A. Carcinogenesis 2000;21:353–359. [PubMed: 10688855]
8. Turteltaub KW, Dingley KH. Toxicol Lett 1998;102-103:435–439. [PubMed: 10022292]
9. Farmer PB, Brown K, Tompkins E, Emms VL, Jones DJ, Singh R, Phillips DH. Toxicol Appl Pharmacol 2005;207:293–301. [PubMed: 15990134]
10. Koc H, Swenberg JA. J Chromatogr B Analyt Technol Biomed Life Sci 2002;778:323–343.
11. Turesky RJ, Vouros P. J Chromatogr B Analyt Technol Biomed Life Sci 2004;802:155–166.
12. Singh R, Farmer PB. Carcinogenesis 2006;27:178–196. [PubMed: 16272169]
13. Paehler A, Richoz J, Soglia J, Vouros P, Turesky RJ. Chem Res Toxicol 2002;15:551–561. [PubMed: 11952342]
14. McLuckey SA, Van Berkel GJ, Goeringer DE, Glish GL. Anal Chem 1994;66:689A–696A.
15. Gangl E, Utkin I, Gerber N, Vouros P. J Chromatogr A 2002;974:91–101. [PubMed: 12458929]
16. Paul W. Agnew Chem Int Ed Engl 1990;29:739–748.

17. Mikesh LM, Ueberheide B, Chi A, Coon JJ, Syka JE, Shabanowitz J, Hunt DF. Biochim Biophys Acta 2006;1764:1811–1822. [PubMed: 17118725]
18. Jackson PE, Scholl PF, Groopman JD. Mol Med Today 2000;6:271–276. [PubMed: 10859563]
19. Chowdhury G, Guengerich FP. Angew Chem Int Ed Engl 2008;47:381–384. [PubMed: 18022988]
20. Andreu V, Pico Y. Curr Anal Chem 2005;1:241–265.
21. Anari MR, Sanchez RI, Bakhtiar R, Franklin RB, Baillie TA. Anal Chem 2004;76:823–832. [PubMed: 14750881]
22. Ma L, Wen B, Ruan Q, Zhu M. Chem Res Toxicol 2008;21:1477–1483. [PubMed: 18549250]
23. Li L, Chiarelli MP, Branco PS, Antunes AM, Marques MM, Goncalves LL, Beland FA. J Am Soc Mass Spectrom 2003;14:1488–1492. [PubMed: 14652195]
24. Turesky RJ, Goodenough AK, Ni W, McNaughton L, LeMaster DM, Holland RD, Wu RW, Felton JS. Chem Res Toxicol 2007;20:520–530. [PubMed: 17316027]
25. Goodenough AK, Schut HA, Turesky RJ. Chem Res Toxicol 2007;20:263–276. [PubMed: 17305409]
26. Liu X, Lovell MA, Lynn BC. Chem Res Toxicol 2006;19:710–718. [PubMed: 16696574]
27. Schwartz JC, Senko MW, Syka JEP. J Am Soc Mass Spectrom 2002;13:659–669. [PubMed: 12056566]
28. Thermo Electron PSB 117. Thermo Electron Corporation; 2006.
29. Bonilla LE, Thakur R, Guzzetta A, Jaffe JD. Appl Note 328. 2006
30. Riter LS, Gooding KM, Hodge BD, Julian RK Jr. Proteomics 2006;6:1735–1740. [PubMed: 16475232]
31. National Toxicology Program. Report on Carcinogenesis. Vol. Eleventh. U.S. Department of Health and Human Services, Public Health Service; Research Triangle Park, N.C.: 2005.
32. Sugimura T, Wakabayashi K, Nakagama H, Nagao M. Cancer Sci 2004;95:290–299. [PubMed: 15072585]
33. Churchwell MI, Beland FA, Doerge DR. Chem Res Toxicol 2002;15:1295–1301. [PubMed: 12387628]
34. Lao Y, Villalta PW, Sturla SJ, Wang M, Hecht SS. Chem Res Toxicol 2006;19:674–682. [PubMed: 16696570]
35. Kanaly RA, Hanaoka T, Sugimura H, Toda H, Matsui S, Matsuda T. Antioxid Redox Signal 2006;8:993–1001. [PubMed: 16771689]
36. Witze ES, Old WM, Resing KA, Ahn NG. Nat Methods 2007;4:798–806. [PubMed: 17901869]
37. Mutlib A, Lam W, Atherton J, Chen H, Galatsis P, Stolle W. Rapid Commun Mass Spectrom 2005;19:3482–3492. [PubMed: 16261644]
38. Lin D, Kaderlik KR, Turesky RJ, Miller DW, Lay JO Jr, Kadlubar FF. Chem Res Toxicol 1992;5:691–697. [PubMed: 1446011]
39. Turesky RJ, Rossi SC, Welti DH, Lay JO Jr, Kadlubar FF. Chem Res Toxicol 1992;5:479–490. [PubMed: 1391614]
40. Frederiksen H, Frandsen H, Pfau W. Carcinogenesis 2004;25:1525–1533. [PubMed: 15059926]
41. Jones CR, Sabbioni G. Chem Res Toxicol 2003;16:1251–1263. [PubMed: 14565767]
42. Ruan Q, Kim HY, Jiang H, Penning TM, Harvey RG, Blair IA. Rapid Commun Mass Spectrom 2006;20:1369–1380. [PubMed: 16557497]
43. Nechev LV, Kozekov ID, Brock AK, Rizzo CJ, Harris TM. Chem Res Toxicol 2002;15:607–613. [PubMed: 12018980]
44. Nechev LV, Harris CM, Harris TM. Chem Res Toxicol 2000;13:421–429. [PubMed: 10813660]
45. Wang H, Rizzo CJ. Org Lett 2001;3:3603–3605. [PubMed: 11678719]
46. Beland FA, Doerge DR, Churchwell MI, Poirier MC, Schoket B, Marques MM. Chem Res Toxicol 1999;12:68–77. [PubMed: 9894020]
47. Beland FA, Churchwell MI, Von Tungeln LS, Chen S, Fu PP, Culp SJ, Schoket B, Gyorffy E, Minarovits J, Poirier MC, Bowman ED, Weston A, Doerge DR. Chem Res Toxicol 2005;18:1306–1315. [PubMed: 16097804]
48. Langouët S, Paehler A, Welti DH, Kerriguy N, Guillouzo A, Turesky RJ. Carcinogenesis 2002;23:115–122. [PubMed: 11756232]

49. Lum A, Le ML. Cancer Epidemiol Biomarkers Prev 1998;7:719–724. [PubMed: 9718225]
50. Hecht SS. Nat Rev Cancer 2003;3:733–744. [PubMed: 14570033]
51. Patrianakos C, Hoffmann D. J Assoc Off Anal Chem 1979;3:150–154.
52. Matsumoto T, Yoshida D, Tomita H. Cancer Lett 1981;12:105–110. [PubMed: 7272995]
53. Chung FL, Nath RG, Nagao M, Nishikawa A, Zhou GD, Randerath K. Mutat Res 1999;424:71–81. [PubMed: 10064851]
54. Beland FA, Kadlubar FF. Environ Health Perspect 1985;62:19–30. [PubMed: 4085422]
55. Swaminathan S, Hatcher JF. Chem Biol Interact 2002;139:199–213. [PubMed: 11823007]
56. Ricicki EM, Soglia JR, Teitel C, Kane R, Kadlubar F, Vouros P. Chem Res Toxicol 2005;18:692–699. [PubMed: 15833029]
57. Chiarelli MP, Lay JO Jr. Mass Spectrom Rev 1992;11:447–493.
58. Jamin EL, Arquier D, Canlet C, Rathahao E, Tulliez J, Debrauwer L. J Am Soc Mass Spectrom 2007;18:2107–2118. [PubMed: 17936011]
59. Foiles PG, Miglietta LM, Quart AM, Quart E, Kabat GC, Hecht SS. Carcinogenesis 1989;10:1429–1434. [PubMed: 2502322]
60. Zhang S, Villalta PW, Wang M, Hecht SS. Chem Res Toxicol 2007;20:565–571. [PubMed: 17385896]
61. Yoshida D, Matsumoto T. Cancer Lett 1980;10:141–149. [PubMed: 7006799]
62. Manabe S, Tohyama K, Wada O, Aramaki T. Carcinogenesis 1991;12:1945–1947. [PubMed: 1934275]
63. Vondracek M, Xi Z, Larsson P, Baker V, Mace K, Pfeifer A, Tjalve H, Donato MT, Gomez-Lechon MJ, Grafstrom RC. Carcinogenesis 2001;22:481–488. [PubMed: 11238190]
64. Spivack SD, Hurteau GJ, Jain R, Kumar SV, Aldous KM, Gierthy JF, Kaminsky LS. Cancer Res 2004;64:6805–6813. [PubMed: 15375000]
65. Liu Y, Sundqvist K, Belinsky SA, Castonguay A, Tjalve H, Grafstrom RC. Carcinogenesis 1993;14:2383–2388. [PubMed: 8242870]
66. Stone MP, Cho YJ, Huang H, Kim HY, Kozekov ID, Kozekova A, Wang H, Minko IG, Lloyd RS, Harris TM, Rizzo CJ. Acc Chem Res 2008;41:793–804. [PubMed: 18500830]
67. Nath RG, Ocando JE, Guttenplan JB, Chung FL. Cancer Res 1998;58:581–584. [PubMed: 9485001]
68. Liu X, Lovell MA, Lynn BC. Anal Chem 2005;77:5982–5989. [PubMed: 16159131]
69. Zhang YJ, Hsu TM, Santella RM. Cancer Epidemiol Biomarkers Prev 1995;4:133–138. [PubMed: 7537994]
70. Romano G, Mancini R, Fedele P, Curigliano G, Flamini G, Giovagnoli MR, Malara N, Boninsegna A, Vecchione A, Santella RM, Cittadini A. Anticancer Res 1997;17:2827–2830. [PubMed: 9252724]
71. Gangl ET, Annan MM, Spooner N, Vouros P. Anal Chem 2001;73:5635–5644. [PubMed: 11774901]
72. Grollman AP, Shibutani S, Moriya M, Miller F, Wu L, Moll U, Suzuki N, Fernandes A, Rosenquist T, Medverec Z, Jakovina K, Brdar B, Slade N, Turesky RJ, Goodenough AK, Rieger R, Vukelic M, Jelakovic B. Proc Natl Acad Sci U S A 2007;104:12129–12134. [PubMed: 17620607]
73. Baillie TA. Chem Res Toxicol 2008;21:129–137. [PubMed: 18052111]

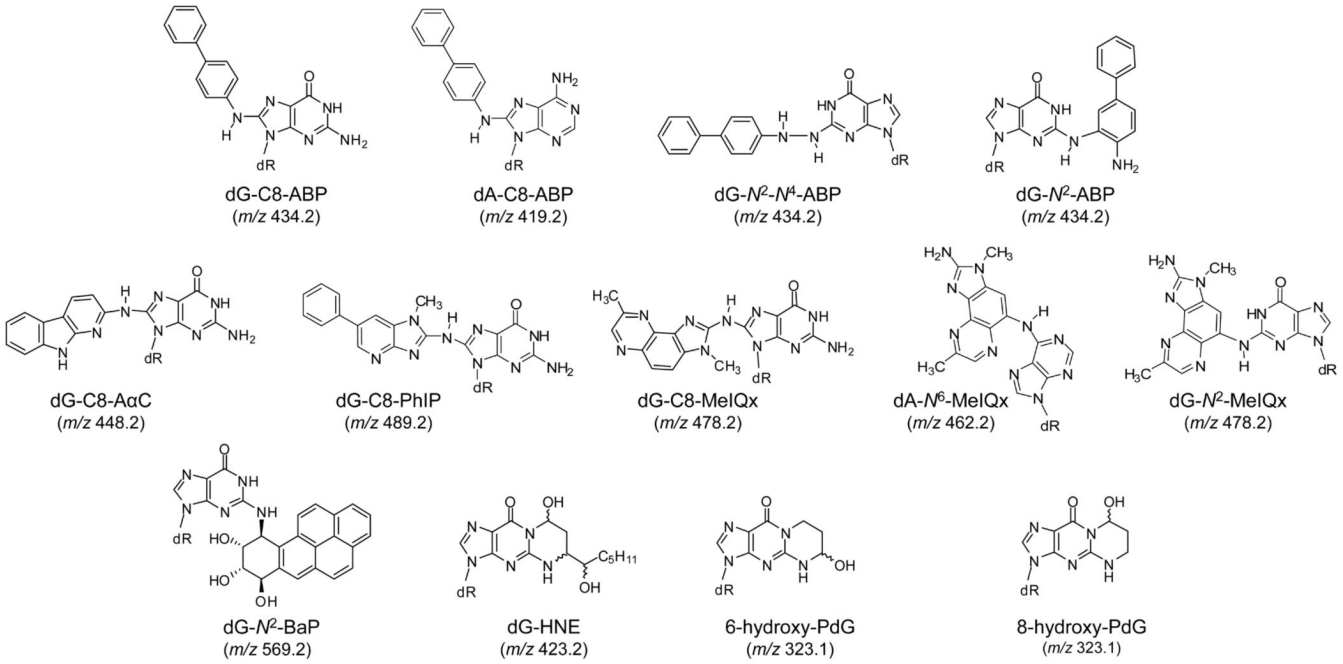

Figure 1.
Structures of DNA adducts under investigation.

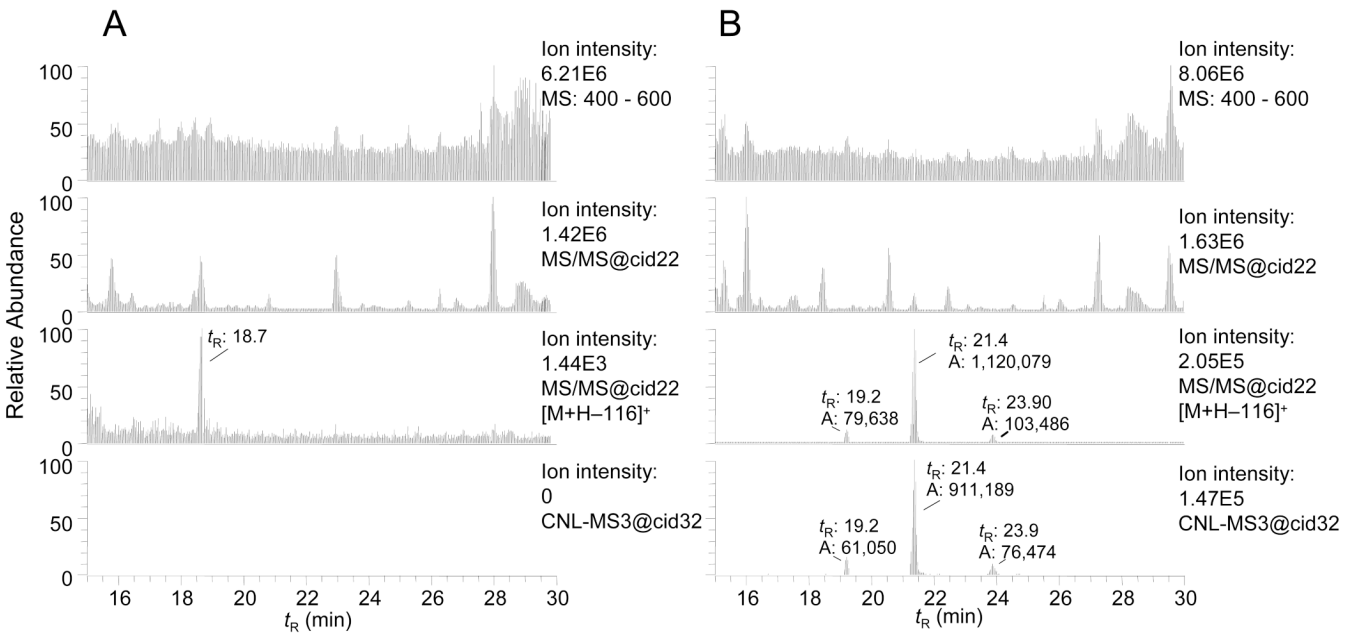

Figure 2.

Global CNL-MS^3 data-dependent scanning of 4-ABP adducts in human hepatocytes, either (A) untreated or (B) 4-ABP-treated (10 μM). The upper chromatograms in each panel displays the full scan mode from 400 to 600 Da. The second chromatogram down is a collection of all MS/MS spectral chromatograms. The third chromatogram displays all of the peaks that are filtered by the CNL $[M+H]^+ \rightarrow [M+H-116]^+$. The bottom chromatogram displays all of the peaks that were detected by the data-dependent CNL-MS^3 scan mode. The respective t_R and area of response of the ion counts are shown.

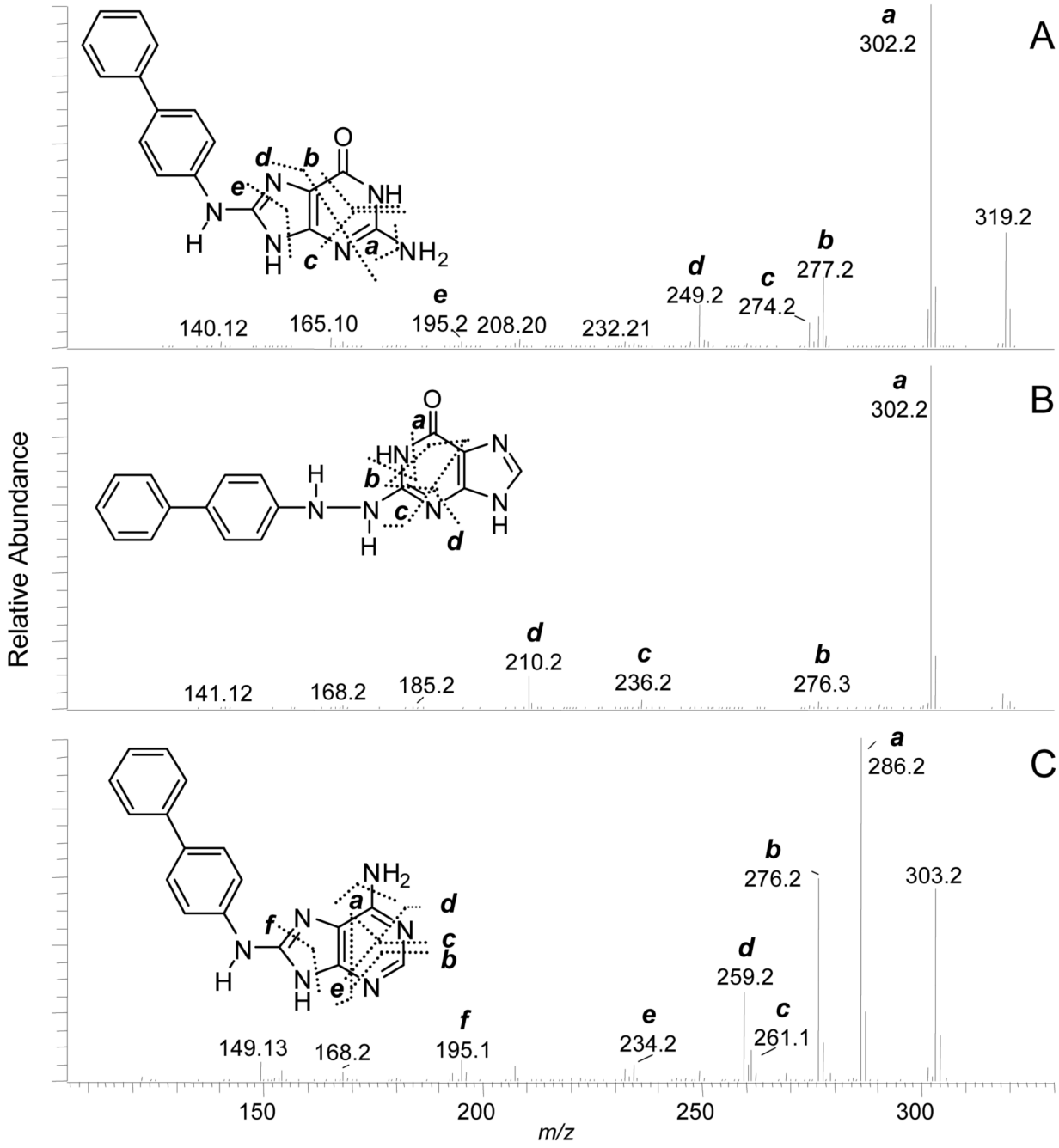

Figure 3.
CNL-MS^3 product ion spectra of (A) dG-C8-ABP, (B) proposed dG-N^2-N^4-ABP adduct, and (C) dA-C8-ABP.

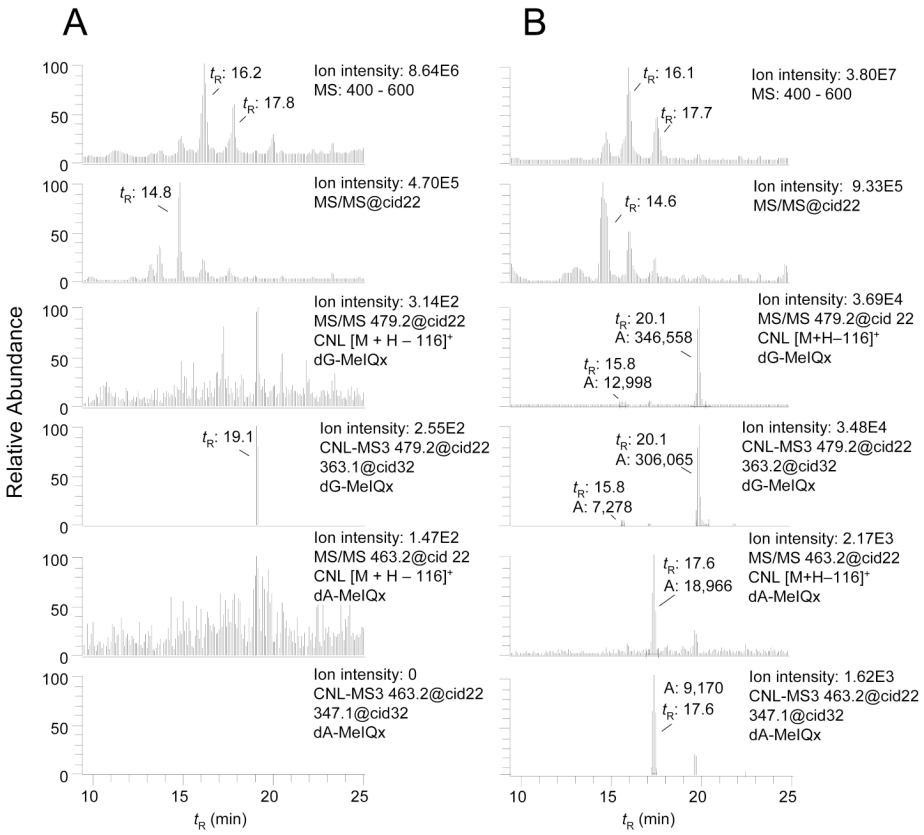

Figure 4.

Targeted data-dependent scanning of DNA adducts in liver of (A) untreated and (B) MeIQx (10 mg/kg) treated rats. The upper chromatogram displays the full scan mode from 400 to 600 Da. The second chromatogram down is a collection of all MS/MS chromatograms. The third chromatogram displays all the peaks at *m/z* 479.1 (dG-MeIQx) that are filtered by the CNL $[M+H]^+ \rightarrow [M+H-116]^+$. The fourth chromatogram displays all the peaks at *m/z* 479.1 (dG-MeIQx) that are detected by the data-dependent CNL-MS^3. The fifth chromatogram displays all the peaks at *m/z* 463.2 (dA-MeIQx) that are filtered by the CNL $[M+H]^+ \rightarrow [M+H-116]^+$. The bottom chromatogram displays all the peaks at *m/z* 463.2 (dA-MeIQx) that are detected by the data-dependent CNL-MS^3. The respective t_R and area of response of the ion counts are shown.

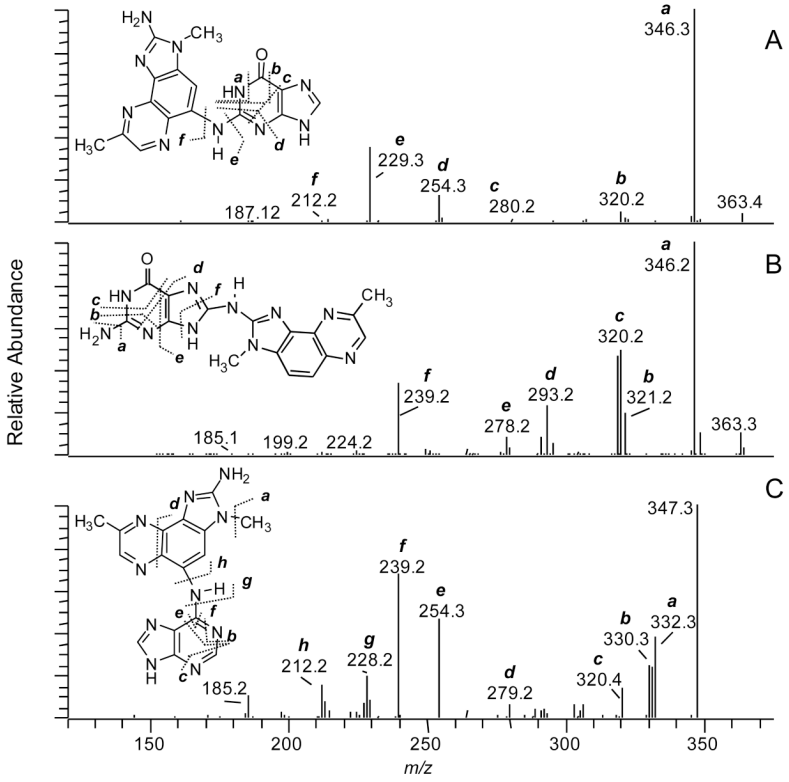

Figure 5.

CNL-MS^3 product ion spectra of (A) dG-*N*^{2}-MeIQx, (B) dG-C8-MeIQx, and (C) the proposed dA-C8-MeIQx.

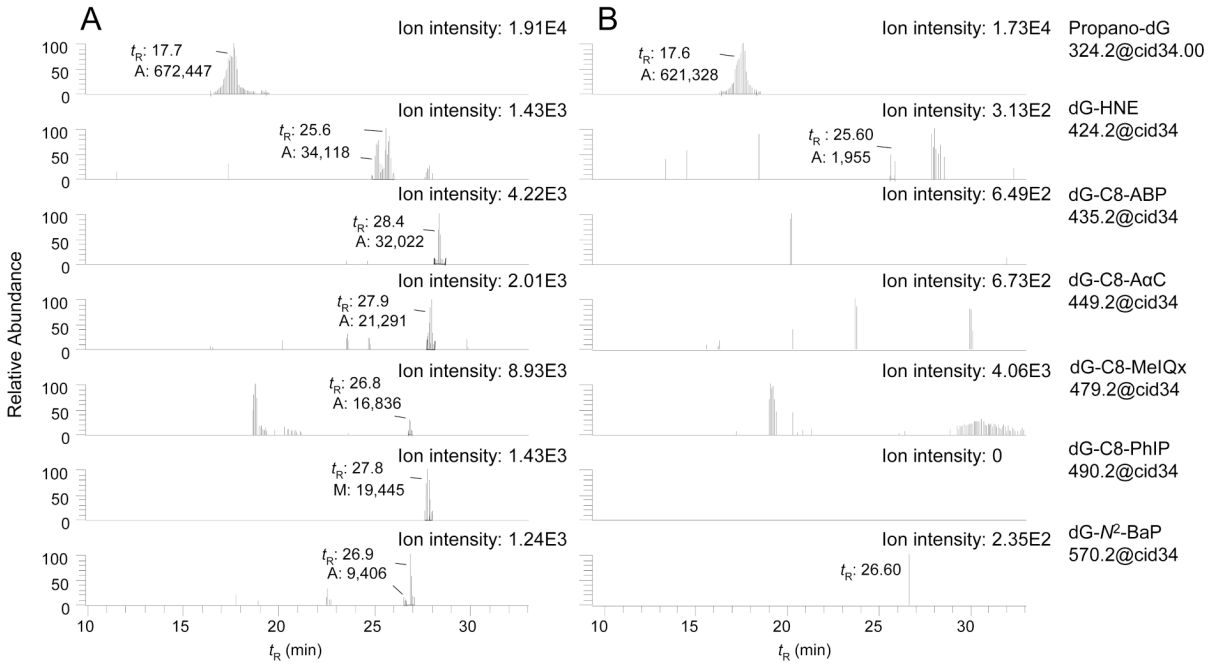

Figure 6.

Targeted data-dependent scanning in CNL-MS^3 of DNA adducts in (A) spiked buccal cells and (B) unspiked buccal cells. The chromatograms show the CNL-MS^3 traces for 6-hydroxy-PdG and 8-hydroxy-PdG (*m/z* 324.2), dG-HNE (*m/z* 424.2), dG-C8-ABP (*m/z* 435.2), dG-C8-AαC (*m/z* 449.2), dG-C8-MeIQx (*m/z* 479.2), dG-C8-PhIP (*m/z* 490.2), and dG-N^2-BaP (*m/z* 570.2); the area of response of the ion counts are shown.

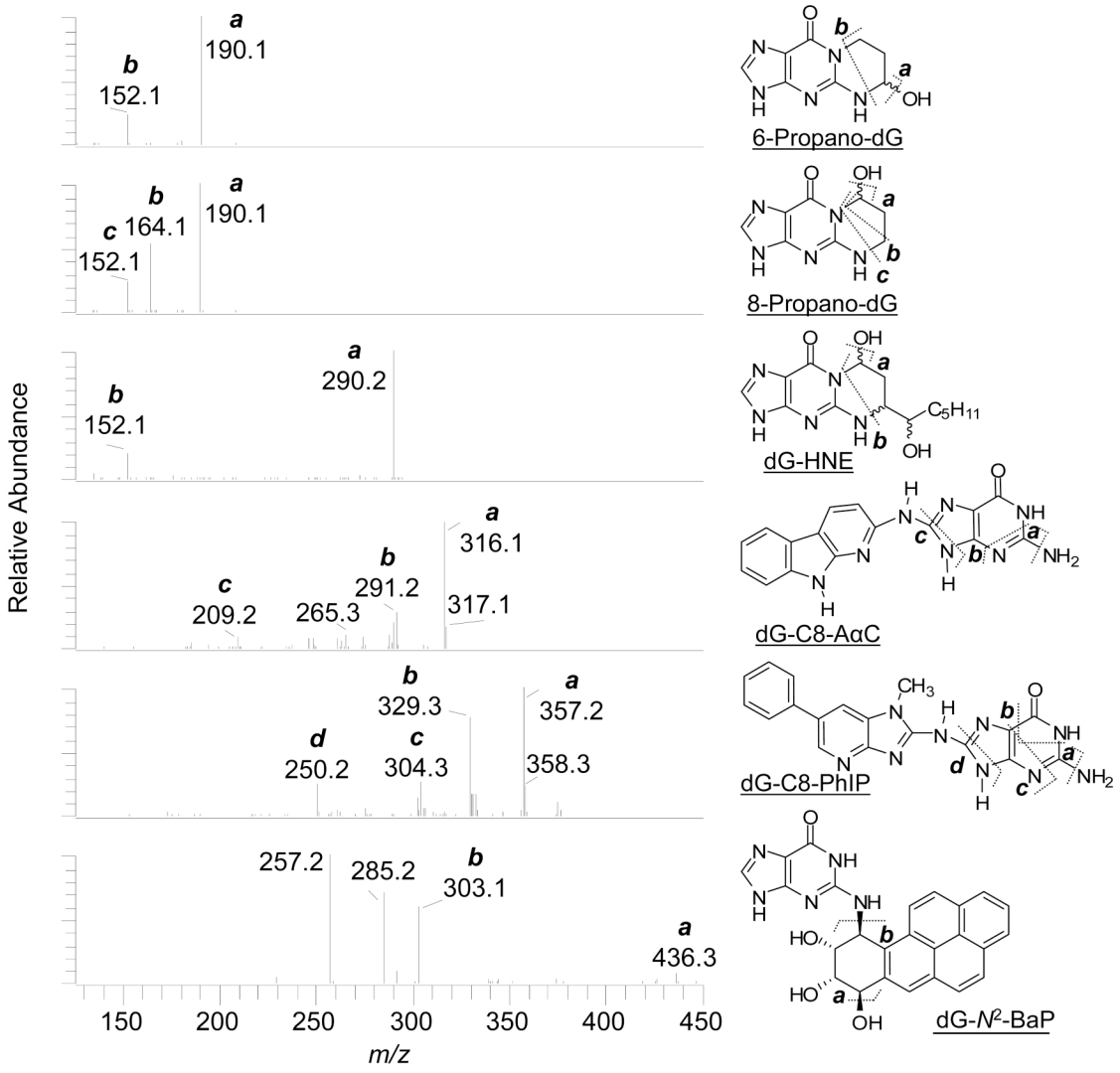

Figure 7.

CNL-MS^3 product ion spectra of DNA adducts recovered from spiked buccal cells and the aglycone adduct structures with proposed mechanisms of fragmentation at the MS^3 scan stage. The product ions of guanyl-*N*^{2}-BaP (*m/z* 454.2) that arise at *m/z* 257.2 and 285.2 are proposed to occur by elimination of H_2O, followed by the expulsion of CO from the tetrahydro-BaP-7,8,9-triol cation species (*m/z* 303) in the ion trap.